Journal of Electronic Materials (2023) 52:7157–7163
https://doi.org/10.1007/s11664-023-10625-1

ORIGINAL RESEARCH ARTICLE

High-Performance Field-Effect Transistor Fabricated on CVD-Grown MoS_2 Monolayers with Indium Contacts

Hina Mustafa[1] · Jahangir Khan[1] · Abdul Sattar[1] · Muhammad Irfan[1] · Sania Gul[2] · Irsa Zalfiqar[3]

Received: 10 January 2023 / Accepted: 17 July 2023 / Published online: 16 August 2023

Abstract

Molybdenum disulfide (MoS_2), an emerging two-dimensional semiconductor material, has been keenly studied for field-effect transistors (FETs). In this work, we explored the optical and electrical properties of FETs fabricated by MoS_2 flakes grown by chemical vapor deposition (CVD) and transferred to the electrodes through propylene carbonate film. Large-area, high-quality and highly crystalline MoS_2 monolayers up to 58 µm are obtained through CVD. Flakes are characterized by optical microscopy, atomic force microscopy, Raman spectroscopy, and photoluminescence analysis. The back-gated measurements are performed in ambient conditions without any encapsulation of the device. The fabricated device reveals *n*-type behavior with high field-effect mobility of 32 cm^2/V s and high current ON/OFF ratio of 10^6. Good ohmic contact is achieved while using indium as source/drain electrodes. The large sized, highly crystalline flakes of MoS_2 and the fabricated device showing high field-effect mobility and ON/OFF ratio make them potential candidates for high-performance nanoelectronics and optoelectronics devices.

Keywords Two-dimensional materials · MoS_2 · chemical vapor deposition · propylene carbonate · field-effect transistor · indium

Introduction

Because of its unique and remarkable electrical properties, graphene has potential for substitution in typical Si-based semiconductor devices.[1] Although graphene has extraordinary high carrier mobility,[2] its zero band gap limits its use in logic applications. Inspired by the invention of graphene monolayers, transition metal dichalcogenides (TMDs) such as MoS_2, $MoSe_2$, WS_2 and WSe_2 have gained significant consideration for their excellent potentials in research fields of nanotechnology, microelectronics, photonics, and optoelectronics.[3,4] TMDs possess a layered hexagonal structure having a dangling bond-free surface, excellent thermal conductivity, and stability.[5] Among these TMDs, MoS_2 has been studied widely as it exhibits excellent flexibility, electrical and optical properties.[6] In MoS_2, each Mo atom is covalently bonded to two sulfur atoms. This covalent bonding provides great mechanical strength to MoS_2. MoS_2 has an outstanding ON/OFF ratio of about 10^8 and carrier mobility almost equal to 200 cm^2/V s at standard temperature.[7] MoS_2 has a tunable bandgap, from 1 to 2 eV.[8,9] The bandgap of MoS_2 changed from an indirect to a direct one from bulk MoS_2 to monolayer MoS.[9] Monolayer MoS_2 has a direct bandgap of 1.9 eV which makes it suitable for use in electronic and optoelectronic devices.[10]

Thin layers of MoS_2 can be obtained by various methods such as mechanical exfoliation,[7] liquid exfoliation,[11] chemical vapor deposition (CVD),[12] sulfurization,[13] physical vapor deposition,[14] and hydrothermal[15] and electrochemical synthesis.[16] Flakes of high quality can be achieved by exfoliation, but these flakes are randomly dispersed, limiting control of the number of layers of MoS_2. Hence, these methods are not designed for large-scale device fabrication. By synthesis, MoS_2 forms nanotubes (one-dimensional) or closed (zero-dimensional) structures. It is very rare to obtain large-area, high-quality, layer-controlled and high-yield MoS_2 for bulk fabrication of devices with excellent

✉ Abdul Sattar
asattar@cuilahore.edu.pk

1 Department of Physics, COMSATS University Islamabad, Lahore Campus, Defence Road, Lahore 54000, Pakistan

2 Department of Chemistry, Islamia College University, Peshawar, Pakistan

3 Department of Optical Engineering, Sejong University, Seoul 30000, South Korea

electrical properties. CVD is used extensively to produce large-area layers of MoS_2 with control over the number of layers, but this method does not ensure the high quality of the flakes. Enhanced scalability has been reported by using various methods, for example sulfurization of molybdenum and its oxides, vapor-liquid growth by using powder MoO_3 and sulfur, thermal decomposition of ammonium thiomolybdates, and vapor-solid growth of MoS_2 monolayers by using powder of MoS_2.[17] In emerging CVD methods, sulfurization is done after spin coating of a solution of metal on a substrate.[18] Sulfurization with sulfur vapor has been demonstrated to be useful for fabricating sputtered-multilayer MoS_2 films with an approximately 4-nm thickness with enhanced mobility.[19]Monolayers of MoS_2 have been achieved by CVD on a mica substrate. A 7.5-nm-thick MoS_2 film was produced. Except for monolayers, no other layers of MoS_2 have been fabricated. With the help of a nucleation promoter, perylene-3,4,9,10-tetracarboxylic acid tetrapotassium salt (PTAS), a highly crystalline and uniform monolayer of MoS_2 has been fabricated.[20] However, it is very hard to use this monolayer uniformly on a large substrate. Wafer-scale monolayers of MoS_2 have been synthesized which exhibit on/off ratios ranging from 10^5 to 10^8 and carrier mobility up to 1.2 cm^2/V s.[21] A recent work investigating field-effect transistors (FETs) fabricated on monolayer MoS_2 produced by CVD showed carrier mobility of 1.45 cm^2/V s with an ON/OFF ratio of 10^4.[22] MoS_2 FETs fabricated by mechanical exfoliation have shown good carrier mobility, but FETs based on CVD-grown MoS_2 exhibited low electrical performance. Growing a layer-controlled, contamination-free, high-quality, large-scale MoS_2 films for nano-devices with excellent performance is still challenging. Moreover, no optimized parameters and methods have been reported for the growth of monolayer MoS_2.

In this work, we fabricated uniform, highly crystalline, large-area, high-quality monolayers of MoS_2 by CVD on SiO_2 substrates. Atomic force microscopy (AFM), Raman spectroscopy, and photoluminescence (PL) analysis confirmed that our monolayers of MoS_2 are highly scalable, uniform, and crystalline in nature. We also fabricated FETs on CVD-synthesized monolayer MoS_2 films which exhibited an on/off ratio of 10^6 with comparative carrier mobility of 32 cm^2/V s. The contact between the metal electrodes and the MoS_2 becomes one of the most critical aspects restricting device performance. Good ohmic contact is attained when we use indium (In) as electrodes, which improves the performance of the MoS_2-based FETs. Our research work demonstrates that excellent electrical performance of devices based on MoS_2 can be achieved by controlled growth of large-area and high-quality MoS_2 films.

Experimental Setup

MoS_2 Synthesis

Figure 1 demonstrates the setup of the experiment. Thin films of MoS_2 are grown on O_2 plasma treated 100 nm SiO_2/Si substrates in 2-zone CVD with 5 cm quartz. The substrate was pre-treated with O_2 plasma for 120 seconds at 110 W to attain a hydrophilic surface. MoO_3 and sulfur powders purchased from Sigma-Aldrich are used as precursors. Two milligrams of MoO_3 powder was taken in a quartz boat with the substrate in a face-down position arranged on the top of boat. Next, 300 mg of sulfur powder was placed in a separate boat. A distance of 15 cm was maintained between boats containing the MoO_3 and sulfur powder. Sulfur was placed in an upstream position in the furnace. Thin layers of MoS_2 were grown at 750°C under 500 sccm Ar flow.

The shape, density, and growth of the MoS_2 flakes were observed by optical microscopy (OM). The uniformity,

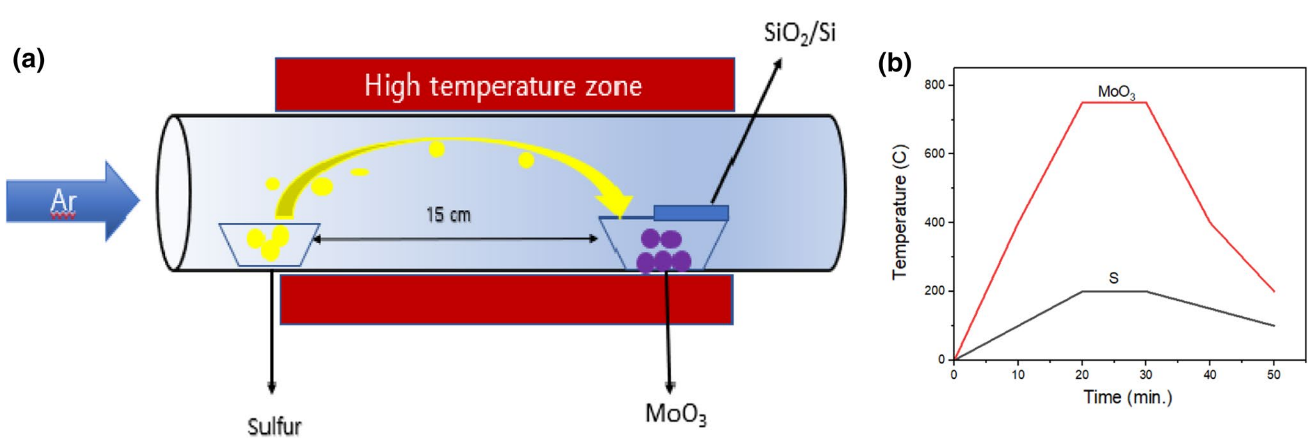

Fig. 1 (a) Schematic diagram of the CVD setup for growth of MoS_2. (b) Temperature profile of S and MoO_3 during growth process.

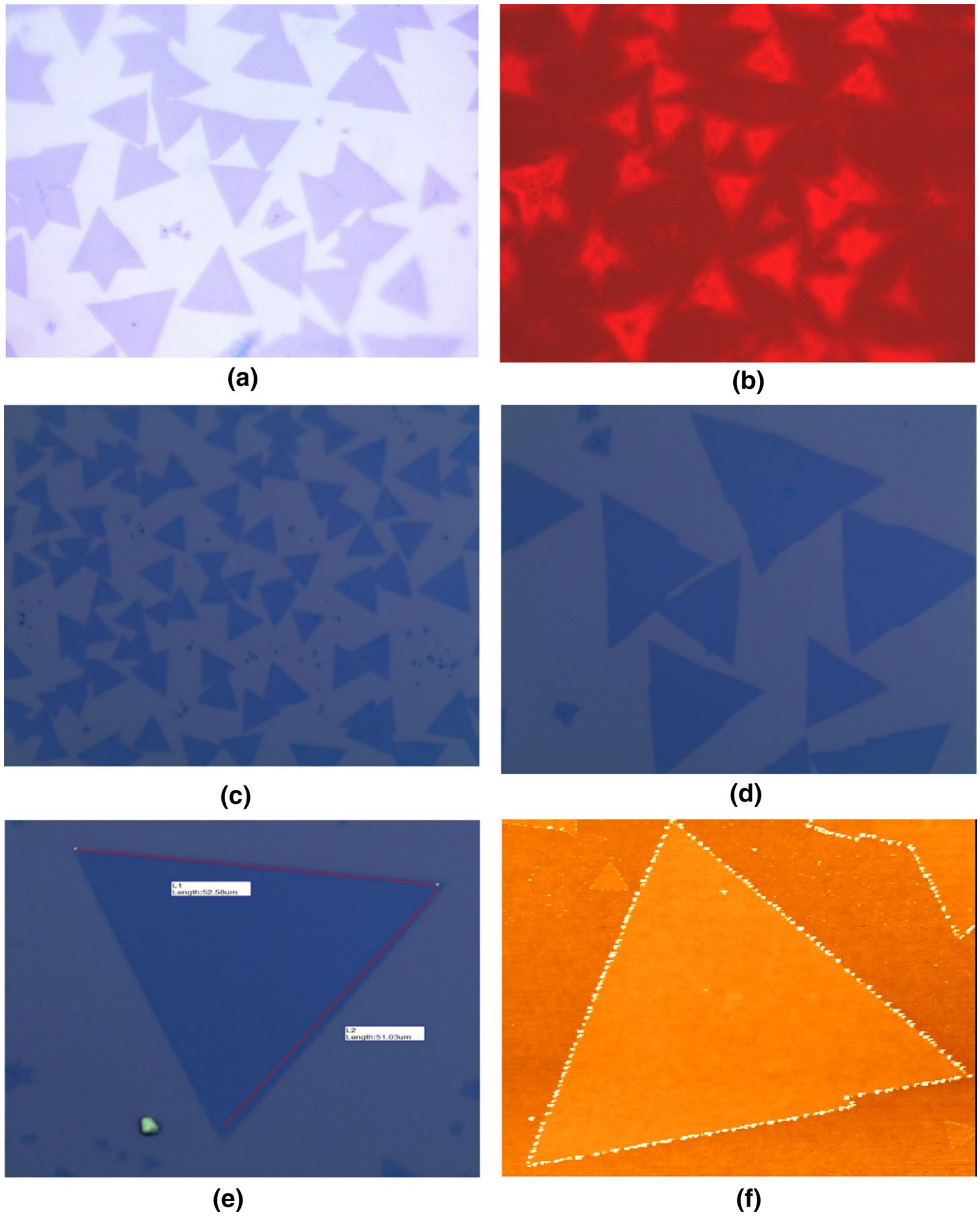

Fig. 2 (a) OM image of MoS_2 flakes. (b) PL image of MoS_2 flakes. (c, d) Density of MoS_2 monolayer flakes. (e) Area of MoS_2 monolayer flake. (f) AFM image of MoS_2 flake.

smoothness and surface structure were examined by a Nano-Magnetics ezAFM system. Raman and PL analysis of MoS_2 flakes were performed using a Renishaw inVia confocal Raman microscope system with an objective lens of 100× with numerical aperture of 0.75 A. continuous wave laser of 532 nm with power of 1 mW was used. Integration time of 0.3 s was used for Raman spectra and 0.02 for PL analysis.

Device Fabrication and Characterizations

The back-gated FET was fabricated by transferring the CVD-grown MoS_2 monolayer on the SiO_2/Si substrate, and Au/In metal electrodes were deposited on it by optical lithography. A total of 80 nm of Au was deposited on 20 nm indium (In) to make electrodes. The MoS_2 flakes synthesized via CVD were relocated onto a SiO_2/Si substrate using a pick-up technique involving the application of propylene carbonate (PC). The PC solution was made by combining

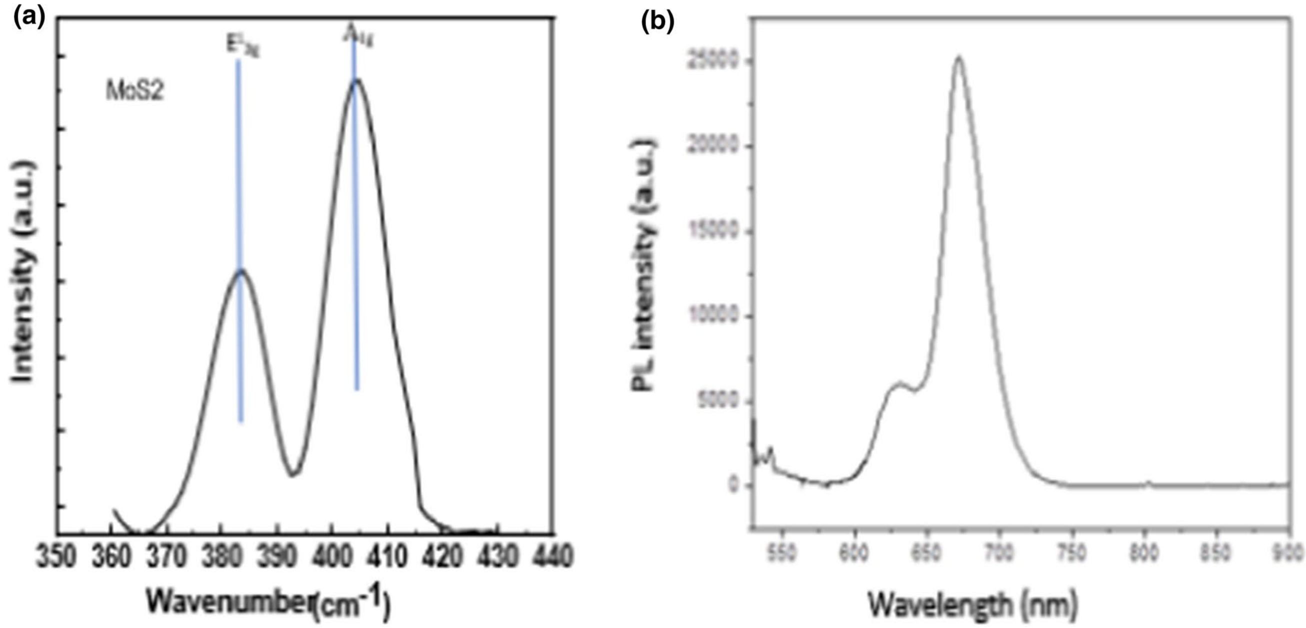

Fig. 3 (a) Raman spectra of MoS_2. (b) PL spectra of MoS_2.

methoxybenzene with PC particles at a mass fraction of around 10%. PC solution was drop-cast on the SiO_2/Si substrate containing CVD-grown MoS_2 flakes. The PC solution was hardened into the PC film by placing it on a hot plate for 10 min at 110°C. The PC film worked as a stamp and carried the MoS_2 layers out of the substrate. Then this PC film was moved to the targeted substrate. At 80°C, the PC film loosened its adhesion and MoS_2 layers were transferred on the desired substrate by removing the PC film. The transfer characteristics of the MoS_2 -based FET were measured with a Keithley 2400 source meter.

Results and Discussion

Optical Characterization

Figure 2a presents the OM images of CVD-grown MoS_2 flakes with triangular shape. PL images of MoS_2 flakes can be seen in Fig. 2b. In Fig. 2c and d the density of the CVD-grown MoS_2 flakes can be seen. We observed maximum crystal size up to 58 µm for this growth. The OM image of a MoS_2 triangle with edges longer than 52.58 µm can be seen in Fig. 2e. In Fig. 2f, a smooth, uniform, highly crystalline and large-area layer structure of MoS_2 flake can be observed with AFM.

Figure 3a presents the Raman spectra of MoS_2. Most significantly, the Raman spectra of MoS_2 show two prominent peaks of MoS_2. Two non-resonant characteristic peaks of MoS_2 are found. These two peaks are dominated by two vibrational modes. $E^1{}_{2g}$ (in-plane vibration) is due to the in-plane vibration of two sulfur atoms with Mo atoms. The $E^1{}_{2g}$ mode appeared at 382 c/m. The A_{1g} mode (out of plane) refers to the out-of-plane vibrations of sulfur atoms in opposite directions. The A_{1g} mode is observed at 404 c/m. These two modes are very sensitive to the thickness of the MoS_2 structure. The thickness and number of layers of MoS_2 are determined by the peak positions of these two modes. The difference between these two peaks tells us about the number of layers of MoS_2. The difference between these two peaks, observed from our Raman spectra, is $A_{1g} - E^1{}_{2g} = 405 - 385 = 20$ c/m and ratio of $A_{1g}/E^1{}_{2g} = 1.057 \approx 1$. The difference of 20 c/m shows that our MoS_2 is monolayer.[23,24] Figure 3b presents the PL spectra of MoS_2. Excitons are the electron-hole pairs which are formed by optical excitation of electrons from valence band to conduction band when MoS_2 is exposed to laser of energy below than 670 nm. As these excited electrons are unstable, they come back from the conduction band to the valence band and relax. In the relaxation state, these electrons recombine with the holes produced in the valence band after their excitation. Radiation is induced because of this recombination. As a result, we observed various peaks of MoS_2 in its PL spectra. Two

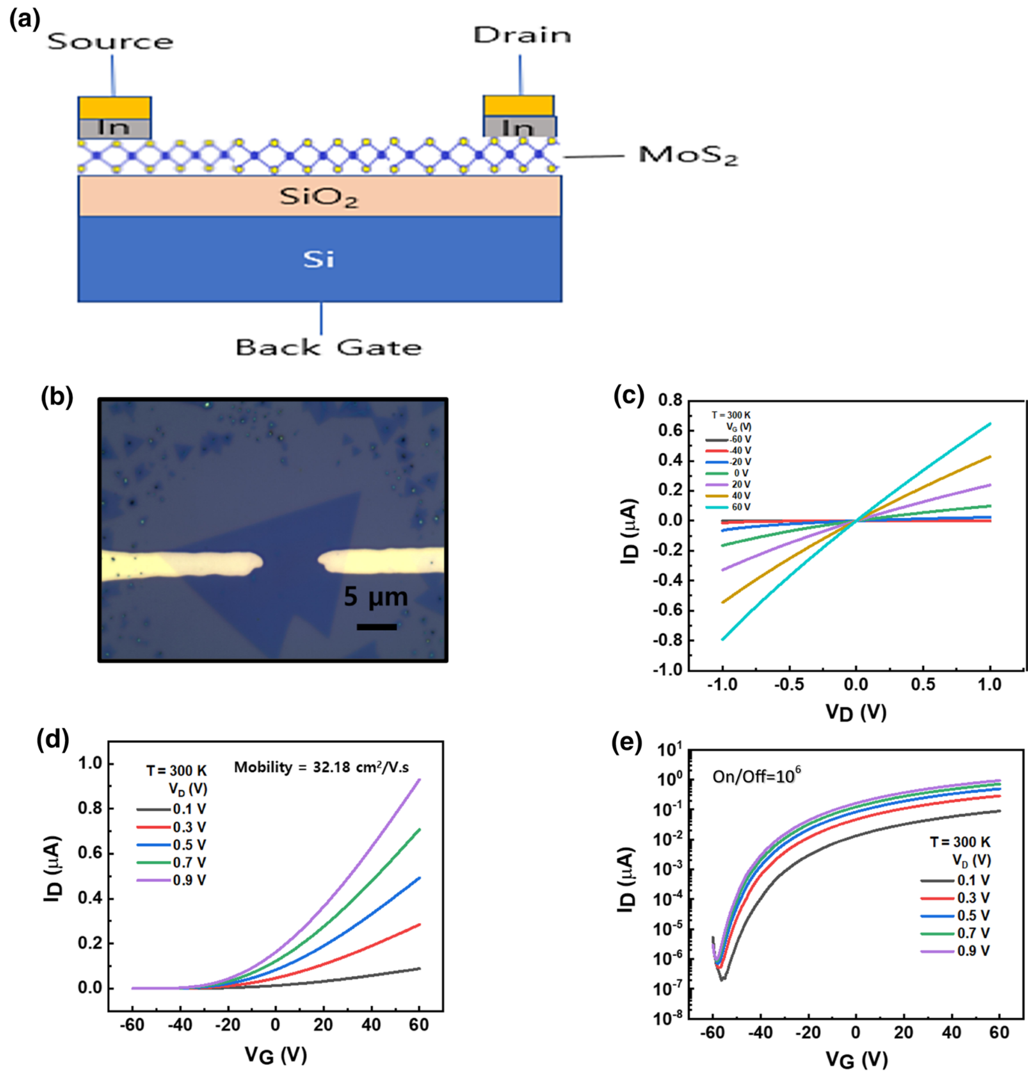

Fig. 4 (a) Cross-sectional diagram of CVD-grown MoS_2 -based FET device. (b) Optical image of fabricated MoS_2 -based FET. (c) Output curves of device by sweeping the V_G from −60 to 60 V. (d, e) Transfer characteristics (I_D–V_G) of monolayer MoS_2-based FET.

well-defined peaks are observed in bare MoS_2 spectra at 1.84 eV and 2.08 eV. These peaks are referred to as A exciton and B exciton, respectively. These peaks demonstrate the exciton formation, and this difference in energy between these two peaks is attributable to the spin-orbit splitting of the valence band.[25]

Electrical Characterization

Figure 4a shows a cross-sectional illustration of the CVD-grown MoS_2-based FET device. The device is fabricated on a SiO_2/Si substrate. SiO_2 with a thickness of 300 nm acts as the gate oxide layer deposited on 500-nm-thick Si. It acts as a back gate to control the fabricated FET. The channel length L_C of the active region is 5 µm and channel width W_c is 6 µm. Figure 4b shows the optical image of the fabricated MoS_2-based FET. Figure 4c, d demonstrates the output and transfer characteristics of the monolayer MoS_2-based FET in contact with In. Output curves of the FET were obtained by taking the Vg from −60 V to 60 V. Good ohmic contact with In was achieved. All electrical measurements were taken in ambient conditions. It is obvious from the transfer curve in Fig. 3d that MoS_2-based FET exhibits *n*-type behavior. From the saturation region of the on-state conducting channel, threshold voltage V_{TH} is defined. V_{TH} is obtained from the intercept made from linear extrapolation on the I_D–V_G graph. FET is usually in the on state when $V_G = 0$ V, which represents the collective conduction of electrons. Figure 3e represents the $I_D - V_G$ curves demonstrating the distinct *n*-type characteristics with ON/OFF = 10.[6]

The field-effect mobility of the MoS_2 -based FET is obtained by using the following equation.

$$\mu_{\mathrm{eff}} = \left(\frac{L}{\mathrm{C_{0x}WV_{ds}}}\right)\left(\frac{d\mathrm{I_{ds}}}{d\mathrm{V_{gs}}}\right)$$

where μ_{FE} is field-effective mobility, g_m is transconductance $= \frac{\partial Id}{\partial Vgs}$, L_c is the length of the channel, C_{go} is the capacitance of the gate oxide, V_D is the drain voltage and W_c is the width of the channel. $C_{go} = \varepsilon_{g0} / t_{og}$ where ε_{go} is the dielectric constant of the gate oxide and t_{og} is the thickness of the gate oxide. This device shows good electronic performance. High mobility of 32 cm^2/V s and an ON/OFF ratio of 10^6 is attained, which is comparatively higher than the previous reported devices fabricated on CVD-grown MoS_2 monolayers.[22,26,27]

Conclusion

We have demonstrated the optical and electronic properties of a FET device based on MoS_2 flakes grown by CVD. A uniform, highly crystalline, large-area, high-quality monolayer of MoS_2 is achieved by CVD on SiO_2 substrates. Electrodes are fabricated by optical lithography and MoS_2, grown by CVD, is transferred through PC film. AFM, Raman, PL, and back-gated measurements are performed in ambient conditions without any encapsulation of the device. The fabricated device reveals *n*-type behavior with high field-effect mobility of 32 cm^2/V s and high current ON/OFF ratio of 10^6. Good ohmic contact is achieved when using In as source/drain electrodes. The large-sized, highly crystalline flakes of MoS_2 and the fabricated device showing high field-effect mobility and ON/OFF ratio make them potential candidates for high-performance nanoelectronic and optoelectronic devices.

Conflict of interest The authors declare that they have no conflict of interest.

References

1. K.S. Novoselov, D. Jiang, F. Schedin, T. Booth, V. Khotkevich, S. Morozov, and A.K. Geim, Two-dimensional atomic crystals. *Proc. Natl. Acad. Sci.* 102(30), 10451 (2005).
2. K.S. Novoselov, L. Colombo, P. Gellert, M. Schwab, and K. Kim, A roadmap for graphene. *Nature* 490(7419), 192 (2012).
3. G. Cunningham, U. Khan, C. Backes, D. Hanlon, D. McCloskey, J.F. Donegan, and J.N. Coleman, Photoconductivity of solution-processed MoS_2 films. *J. Mater. Chem. C* 1(41), 6899 (2013).
4. Y. Gong, J. Lin, X. Wang, G. Shi, S. Lei, Z. Lin, X. Zou, G. Ye, R. Vajtai, and B.I. Yakobson, Vertical and in-plane heterostructures from WS_2/MoS_2 monolayers. *Nat. Mater.* 13(12), 1135 (2014).
5. Z. Lin, C. Wang, and Y. Chai, Emerging group-VI elemental 2d materials: preparations, properties, and device applications. *Small* 16(41), 2003319 (2020).
6. O. Lopez-Sanchez, D. Lembke, M. Kayci, A. Radenovic, and A. Kis, Ultrasensitive photodetectors based on monolayer MoS_2. *Nat. Nanotechnol.* 8(7), 497 (2013).
7. B. Radisavljevic, A. Radenovic, J. Brivio, V. Giacometti, and A. Kis, Single-layer MoS_2 transistors. *Nat. Nanotechnol.* 6(3), 147 (2011).
8. Z. Yu, Z.Y. Ong, S. Li, J.B. Xu, G. Zhang, Y.W. Zhang, Y. Shi, and X. Wang, Analyzing the carrier mobility in transition-metal dichalcogenide MoS_2 field-effect transistors. *Adv. Funct. Mater.* 27(19), 1604093 (2017).
9. H.V. Phuc, N.N. Hieu, B.D. Hoi, N.V. Hieu, T.V. Thu, N.M. Hung, V.V. Ilyasov, N.A. Poklonski, and C.V. Nguyen, Tuning the electronic properties, effective mass and carrier mobility of MoS_2 monolayer by strain engineering: first-principle calculations. *J. Electron. Mater.* 47, 730 (2018).
10. R. Sundaram, M. Engel, A. Lombardo, R. Krupke, A. Ferrari, P. Avouris, and M. Steiner, Electroluminescence in single layer MoS_2. *Nano Lett.* 13(4), 1416 (2013).
11. K.G. Zhou, N.N. Mao, H.X. Wang, Y. Peng, and H.L. Zhang, A mixed-solvent strategy for efficient exfoliation of inorganic graphene analogues. *Angew. Chem.* 123(46), 11031 (2011).
12. Y. Zhan, Z. Liu, S. Najmaei, P.M. Ajayan, and J. Lou, Large-area vapor-phase growth and characterization of MoS_2 atomic layers on a SiO_2 substrate. *Small* 8(7), 966 (2012).
13. H.Y. Jeong, Y. Jin, S.J. Yun, J. Zhao, J. Baik, D.H. Keum, H.S. Lee, and Y.H. Lee, Heterogeneous defect domains in single-crystalline hexagonal WS_2. *Adv. Mater.* 29(15), 1605043 (2017).
14. S. Helveg, J.V. Lauritsen, E. Lægsgaard, I. Stensgaard, J.K. Nørskov, B. Clausen, H. Topsøe, and F. Besenbacher, Atomic-scale structure of single-layer MoS_2 nanoclusters. *Phys. Rev. Lett.* 84(5), 951 (2000).
15. Y. Peng, Z. Meng, C. Zhong, J. Lu, W. Yu, Y. Jia, and Y. Qian, Hydrothermal synthesis and characterization of single-molecular-layer MoS_2 and $MoSe_2$. *Chem. Lett.* 30(8), 772 (2001).
16. Q. Li, J. Newberg, E. Walter, J. Hemminger, and R. Penner, Polycrystalline molybdenum disulfide (2H–MoS_2) nano-and microribbons by electrochemical/chemical synthesis. *Nano Lett.* 4(2), 277 (2004).
17. X. Li and H. Zhu, Two-dimensional MoS_2: properties, preparation, and applications. *J. Mater.* 1(1), 33 (2015).
18. J. Pütz and M.A. Aegerter, Liquid film deposition of chalcogenide thin films. *J. Sol-Gel Sci. Technol.* 26(1), 807 (2003).
19. K. Matsuura, T. Ohashi, I. Muneta, S. Ishihara, K. Kakushima, K. Tsutsui, A. Ogura, and H. Wakabayashi, Low-carrier-density sputtered MoS_2 film by vapor-phase sulfurization. *J. Electron. Mater.* 47, 3497 (2018).
20. Y.C. Kim, Y.H. Ahn, S. Lee, and J.-Y. Park, Large-area growth of high-quality graphene/MoS_2 vertical heterostructures by chemical vapor deposition with nucleation control. *Carbon* 168, 580 (2020).
21. F.K. Perkins, A.L. Friedman, E. Cobas, P. Campbell, G. Jernigan, and B.T. Jonker, Chemical vapor sensing with monolayer MoS_2. *Nano Lett.* 13(2), 668 (2013).
22. H. Şar, A. Özden, B. Yorulmaz, C. Sevik, N. Kosku Perkgoz, and F. Ay, A comparative device performance assesment of CVD grown MoS_2 and WS_2 monolayers. *J. Mater. Sci. Mater. Electron.* 29(10), 8785 (2018).

23. C. Lee, H. Yan, L.E. Brus, T.F. Heinz, J. Hone, and S. Ryu, Anomalous lattice vibrations of single-and few-layer MoS_2. *ACS Nano* 4(5), 2695 (2010).
24. H. Li, Q. Zhang, C.C.R. Yap, B.K. Tay, T.H.T. Edwin, A. Olivier, and D. Baillargeat, From bulk to monolayer MoS_2: evolution of Raman scattering. *Adv. Funct. Mater.* 22(7), 1385 (2012).
25. J. Zhang, H. Yu, W. Chen, X. Tian, D. Liu, M. Cheng, G. Xie, W. Yang, R. Yang, and X. Bai, Scalable growth of high-quality polycrystalline MoS_2 monolayers on SiO_2 with tunable grain sizes. *ACS Nano* 8(6), 6024 (2014).
26. S.S. Withanage, H. Kalita, H.-S. Chung, T. Roy, Y. Jung, and S.I. Khondaker, Uniform vapor-pressure-based chemical vapor deposition growth of MoS_2 using MoO_3 thin film as a precursor for coevaporation. *ACS Omega* 3(12), 18943 (2018).
27. S.K. Kang and H.S. Lee, Study on growth parameters for monolayer MoS_2 synthesized by CVD using solution-based metal precursors. *Appl. Sci. Converg. Technol.* 28(5), 159 (2019).

Publisher's Note Springer Nature remains neutral with regard to jurisdictional claims in published maps and institutional affiliations.